ROTOR RESONANCES ANALYSES OF HIGH-SPEED HIGH POWER PERMANENT-MAGNET ELECTRICAL MACHINES

Wedad Alsadiq Alhawil [1], Ali. A. Mehna [2*], Asheraf Eldieb [3], and Tarak Assaleh[4]

[1,2,3] Electrical engineering department, [4]Mechanical engineering department, faculty of engineering, Subratha University.

[*] alimehna@gmail.com

Abstract

High-speed electric machines (HSEMs) have been widely used in many of today's applications. For high-speed machines, in particular, it is very important to accurately predict natural frequencies of the rotor at the design stage to minimize the likelihood of failure. The main goal of this study is examine the design issues and performance of high-speed machines. For permanent-magnet synchronous motors (PMSM) driven by high-frequency drives, the rotor speed is normally above 30 000 rpm and it may exceed 100 000 rpm. This study examined a 7-kw permanent magnet synchronous machine at 200,000 rpm. 3D finite element analysis (ANSYS WORKBENCH 15) was conducted to determine the natural frequencies and rotor patterns of a synchronous high-speed permanent magnetic motor, to assess the impact of leading design parameters, such as length, column diameter, span, bearings, material properties, and to compare the results of the finite element program with the results of analytical methods (i.e. critical speed).

Keywords: PMSM; Finite element analysis; High speed; High power and critical speed.

Introduction

The mechanical design of high-speed electrical machines is a very responsible task because this type of machine is often designed to operate with a speed that is close to the flexural critical speeds. Errors in the prediction of these speeds can lead to unpleasant phenomena such as excessive acoustic noise emissions and catastrophic failures during operation. In fact, one should be sure that extremely harmful and dangerous vibrations would never occur in the operational speed range of the rotor. In order to achieve a long-lasting life of the machine, this kind of accurate analysis must be performed during its design process. The problem of reliable mechanical design of a high-speed rotor is so serious for a high-speed permanent-magnet (PM) machine because it has a more complex construction than a high-speed induction machine (Miller, 1998) and (Tutelea and Pitic, 2005). The high-speed PM machines have some advantages over the high-speed induction machines like the better

utilization factors, the higher power factors and the higher efficiencies. However, the high-speed induction rotor is more mechanically rigid and stiff because of its relatively simple construction, which is mainly structured of solid steel (Longya Xu et al , 2019). In fact, a high-speed PM rotor usually contains PMs, an eddy-current shield and a retaining sleeve (Ayman El-Refaie and Mohamed Osama, 2019). Since they cannot significantly contribute to the rotor stiffness and they increase the rotor mass, these parts may negatively influence the rotor dynamic behavior. This means that the successful mechanical design of a high-speed PM rotor is a big challenge (Kolondzovski, et al, 2010).

The mechanical design of the rotor, which is extremely important to the overall design of the machine, is one of the main factors in determining the final rotor dimensions. The two main constraints that affect a rotor's dimensions are the mechanical stress due to centrifugal force and the elastic instability associated with critical velocities. Therefore, accurate prediction of the natural frequencies of the rotor group and mechanical pressure at an early stage of design is very important (Ram Kumar, et al, 2019).

However, both electromagnetic and mechanical design issues must be considered too. Obviously, accurate prediction of the natural frequencies and the rotor patterns at the design stage is critical, as improper rotor design may lead to excessive acoustic noise emissions, excessive bearing loss, and even catastrophic failure.

To achieve proper and reliable results ANSYS was used. ANSYS is the original and commonly used abbreviation for ANSYS Mechanical or ANSYS Multimedia, general-purpose finite element analysis software. Actually ANSYS Inc. develops a full range of CAE products, but it is perhaps best known for ANSYS Me- Chanel and ANSYS Multi-physics. Academic releases of these commercial products referred to as ANSYS Academic Research, ANSYS Academic Teaching Advanced, Introductory, and so on. All of these products are a general-purpose limited component. The language of ANSYS commands contains several thousands of construction-related commands such as engineering, network, boundary conditions, solution settings and many other features.

Numerical computation techniques have advanced and computing power has increased; these developments contributed to analysis tools in that they are now able to solve problems that are more complex. A real-life engineering problem may involve different physics such as fluid flow, heat transfer, electromagnetism and more others. The goal of most software developers is to include as much of the real world in the simulation they perform as possible. Finite element method has been used to solve engineering problems in all of these areas successfully. The ANSYS aims to simulate the complete real-life engineering problem. The simulation usually begins by using a three-dimensional CAD model to construct a finite element mesh,

then imposing loads and boundary conditions and finally computing the solution to the finite element problem (Vijayaraghavan, and. Dornfeld, 2005).

This paper covered the mechanical design where three-dimensional finite element methods (**ANSYS WORKBENCH 15**) were used. Firstly some simple analytical models were used to help the initial sizing and then more complex three-dimensional finite element models were used to predict the critical speed, and finally the results were compared with those mentioned in (Jason Ede, Zhu, 2002).

The Influence of Rotor's Design

Free-Free Rotor Shaft

The shaft natural frequencies may be calculated analytically from (D. Hartog, 1956) by using equation (1)

$$\omega_n = a_n \sqrt{\frac{EI}{\mu_1 L^4}} \qquad (1)$$

This equation is used to calculate the natural frequencies of the free-free shaft. A modal simulation under a free-free condition can also be carried out by using the mechanical FEM analysis (Jason Ede, Zhu, 2002); it was used throughout this paper to compare the obtained results. In Table (1), the FE and the analytically calculated natural frequencies are compared with the results obtained from (Jason Ede, Zhu, 2002) whereas vibration mode shapes are presented in Figure (1). It is clear that the calculated and predicted values agree very well with the results obtained from (Jason Ede, Zhu, 2002).

Table (1): Natural Frequencies for Circular Shaft.

MODE	Analytical (Hz)	Finite element (Hz)	Measured (Hz)
1^{st} bending	3044	3064.4	2944
2^{nd} bending	8463	8239.7	8256
Rotational	-	-	-

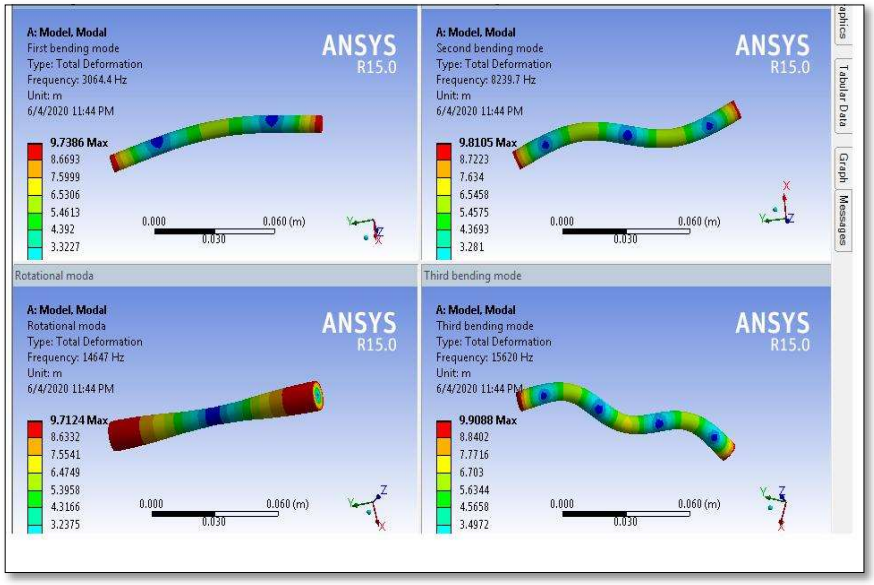

Figure (1): Vibration Modes for a Steel Bar.

Shaft with Long Bearing

The shaft with bearing natural frequencies may be calculated analytically by using equation (2).

$$W_{c1}{}^{2} = \frac{502\,EI}{mL^3} \qquad (2)$$

Table (2) compares the analyzed solution with the FE solution for the natural frequency pattern of the long bearing axis.

Bearing was assumed where the first critical speed occurs at 3835.5 Hz.

Table (2): Comparison Between the Analytical and FE Solution of Natural Frequency Mode of Shaft With Long Bearing.

MODE	Analytical (Hz)	Finite element (Hz)
1^{st}bending	3834.9	3835.5

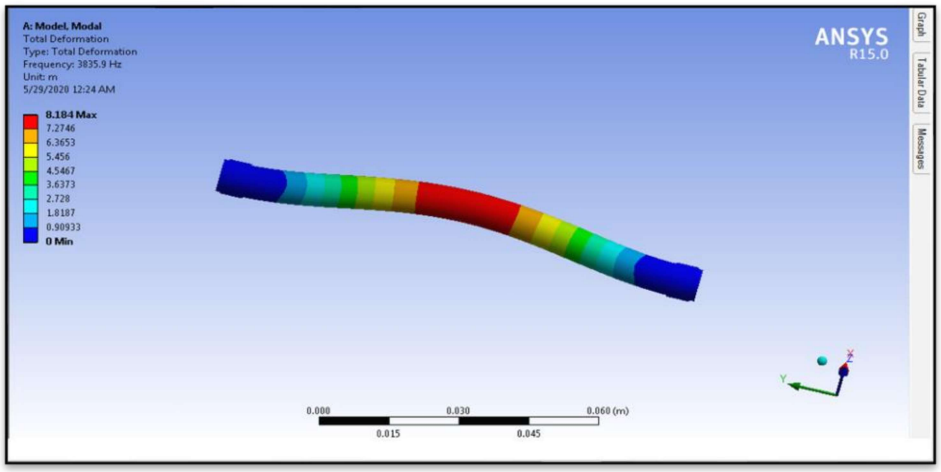

Figure (2): The First Bending Mode of Fixed Two Ends Shaft (X,Y,Z One End and X,Y the Other End) -3835.9Hz.

As can be seen from Table (2), FE predication of the natural frequencies agrees well with the analytical values.

Free-Free Rotor Shaft with End Cap

The rotor shaft with an integral end-cap was considered; Figure (3) shows the vibration mode shapes. Since a key way would lead to an undesirable imbalance, a flat surface was machined on to each side of the shaft in order to locate the laminations. In Table (3), FE predictions of the natural frequencies agree well with the results obtained from [5]. The natural frequencies for the rotor shaft were slightly higher than for the simple circular shaft due to the larger diameter and, hence, stiffness increased, of the active section. This increase would be greater without the end-cap, which increases the mass and thereby reduces the natural frequency.

Table (3): Natural Frequencies of Rotor Shaft/End-Cap.

MODE	Finite element (Hz)	Measured (Hz)
1^{st} bending	2906.6	3200
2^{nd} bending	8483.3	8864
Rotational	11072	-
3^{rd}bending	15122	16032

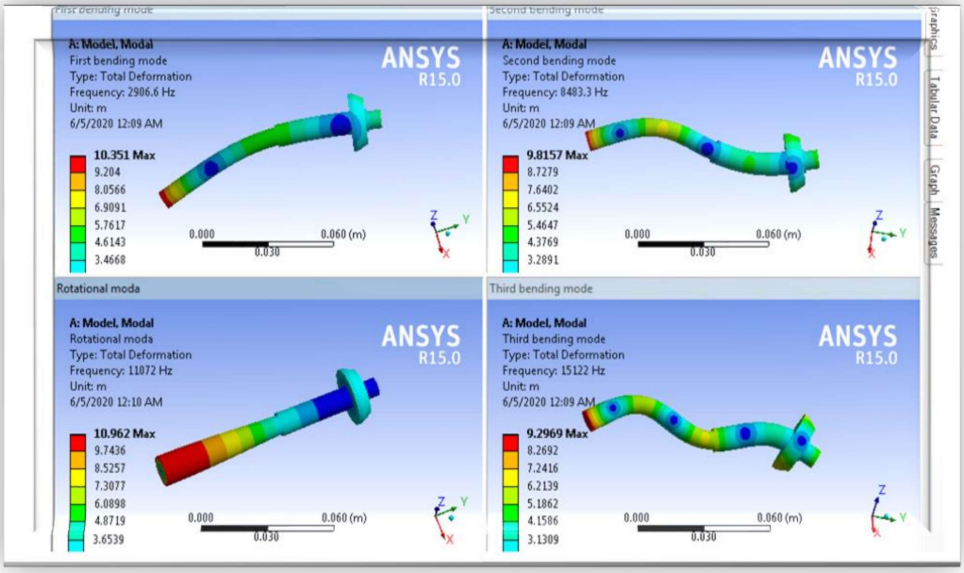

Figure (3): Vibration Modes for a Shaft and End Cap.

Free-Free Shaft with Laminations and End-Caps

Table (4) compares FE predicted natural frequencies with the results obtained from (Jason Ede, Zhu, 2002). As it can be seen, the natural frequencies are significantly lower than the ones in Table (1) due to the addition of the second end-cap, which increased the mass of the rotor rather than axial stiffness. As they increase the mass and make little contribution to the axial stiffness, laminations also reduce the natural frequency,.

Table (4): Natural Frequencies of Rotor Shaft with Laminations and End- Caps.

MODE	Finite element (Hz)	Measured [16 (Hz)
1st bending	2674.2	2752
2nd bending	7782.9	7936
Rotational	8545.4	-
3rd bending	13468	13568

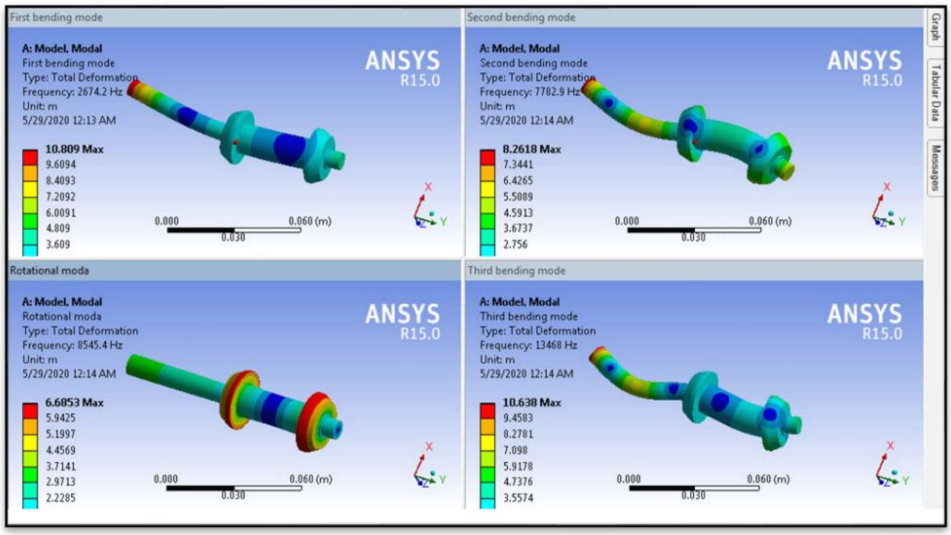

Figure (4): Vibration Modes for Rotor Shaft with Laminations and End-Caps.

Free-Free Rotor Shaft with Laminations, End-Caps, and Magnets

Figure (5) shows the vibration mode shapes, and the comparison of FE predicted natural frequencies are shown in Table (5).

Table (5): Natural Frequencies of Rotor Shaft with Laminations, End-Caps, and Magnets.

MODE	Finite element (Hz)	Measured (Hz)
1^{st} bending	2929.3	3008
2^{nd} bending	11972	12160
Rotational	14976	-
3^{rd}bending	20871	19904

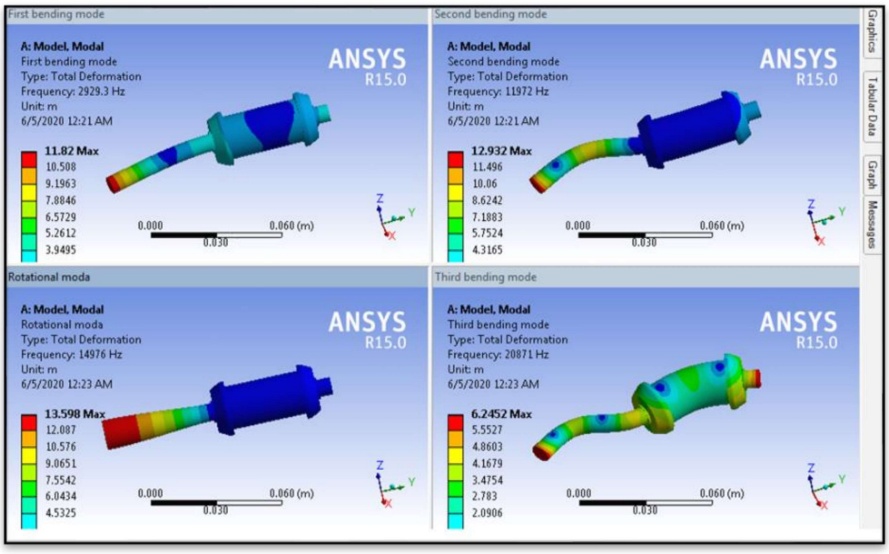

Figure (5): Vibration Modes for Rotor Shaft with Laminations, End-Caps, and Magnets.

Free-Free Assembled Rotor

Table (6) compares the FE and the results obtained in (Jason Ede, Zhu, 2002). The corresponding rotor vibrational modes are shown in Figure (6).

Table (6): Natural Frequencies for Assembled Rotor.

MODE	Finite element (Hz)	Measured [16] (Hz)
1^{st} bending	2824.8	2944
2^{nd} bending	12225	12352
Rotational	15038	15296
3^{rd} bending	27441	20480

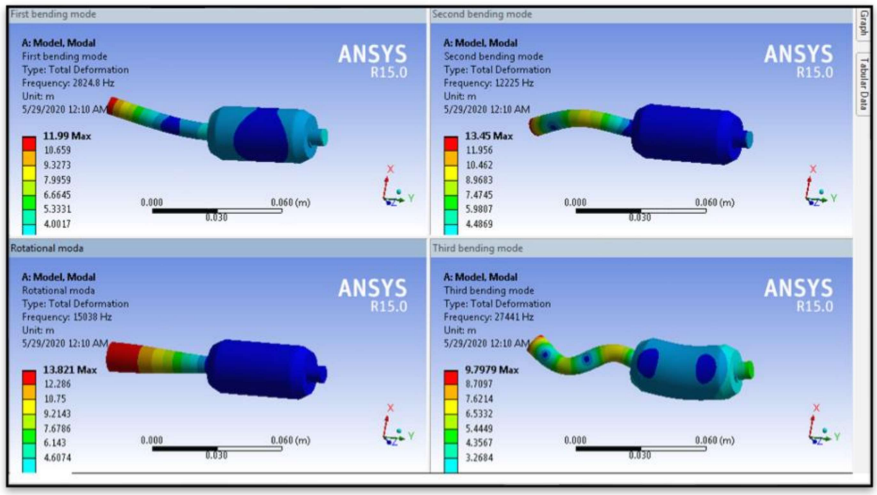

Figure (6): Vibration Mode for Assembled Rotor.

In short, the rotor natural frequencies can be accurately predicted by FEA and the various rotor components affect these frequencies and the modes of the rotor. It was noticed that the addition of the laminations, end-caps, and the carbon fiber over-wrap decreased the natural frequencies of the rotor because they contributed to shaft mass but very little to axial stiffness. On the other hand, the addition of the magnets increased the axial stiffness of the rotor shaft and, hence, increased the natural frequencies significantly; the following Figure (7) shows that.

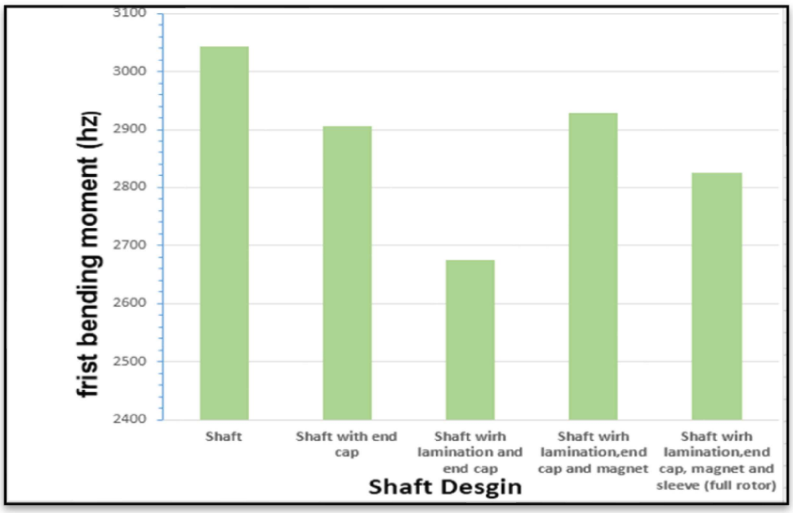

Figure (7): Comparison Between the First Bending Moment for Shaft Design.

Predication of Full Rotor Critical Speed Using 3D FE with Long Bearing

In the 3D FE model, the assembly was modeled as for the shaft alone with one end fixed in x, y and z but in the other end only x and y were fixed.

The Analytical of Rotor with Long Bearing

The shaft natural frequency was calculated analytically using (Eq 3). Uniform shaft, "long" bearings:

$$\mathbf{N_c = \frac{3.57}{L^2}\sqrt{EI/m}} \qquad \mathbf{(3)}$$

Where L, *E, I* and *m* are shaft length, young's module, inertia, and the mass per unit of shaft length, respectively. With a 7.9mm shaft and a 50mm distance between the bearings-long, the first critical speed occurred at 14574.6 Hz., the disc natural frequency was calculated using Eqn. (4)

Central disk of long bearings:

$$\mathbf{N_c = \frac{1}{2\pi\sqrt{\frac{192EI}{mL^3}}}} \qquad \mathbf{(4)}$$

Where *L, E, I* and *m* are shaft length, young's module, inertia, and the mass per unit of shaft length, respectively. With an active length of 49.7 mm and diameter of 20mm, the first critical speed was 96506 Hz direction.

The corresponding vibration modes of the fully assembled rotor are shown in Figure (8).

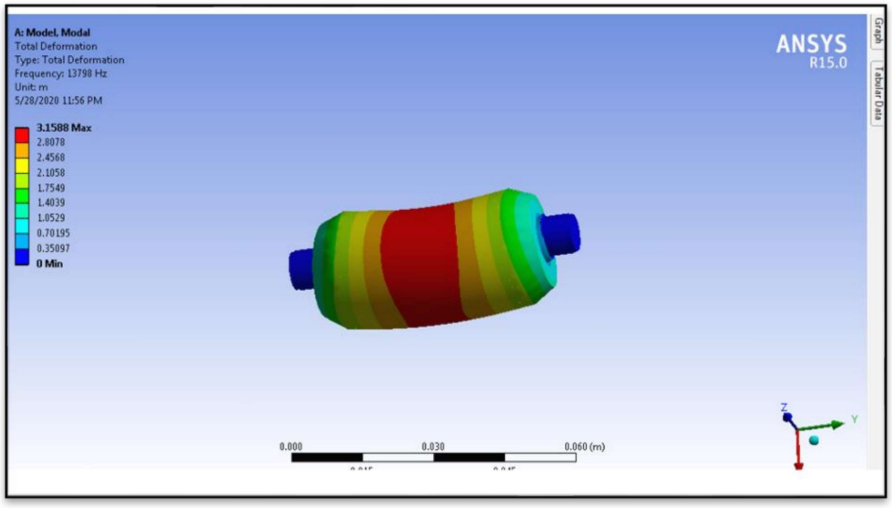

Figure (8): 1st Bending Mode of Full Rotor-13798Hz.

Table (7) compares the FEA with the analytically calculated and predicated natural frequencies.

Table (7): Natural Frequencies of Rotor with Long Bearing.

MODE	Analytical (Hz)	Finite element (Hz)
1st bending	14574.6	13798

The rotor lamination was clamped axially by the two-rotor end clamping rings in order to provide a compression force, which allowed the rotor lamination to act as a single part. The lamination had a very low axial young's module (E_z= 8Gpa) as compared to a solid material (E_z= 161Gpa). However adding lamination to the shaft reduced shaft‘s natural frequency because they increased the mass but added very little to axial stiffness.

Using equations (4), the complete rotor, with an active length of 34mm and a distance of 49.7mm between bearings had a 1st critical speed of 480732 rpm,. This is well above the rated speed of 200,000 rpm. Therefore, critical speeds are not an issue in this design because of the clear margin which enables constructing large machines by making them longer.

Influence of Design Parameters

Axial shaft length has a significant effect on rotor’s natural frequencies. Here, shaft extension was maintained at 15 mm in order to prevent it dominating the vibration mode shapes. The axial length of the active section of the rotor was then reduced as shown in Figure (9). This made the shaft lighter and reduced the stiffness of the central section of the rotor. Figure. (10) Shows the resulting variation of the natural frequencies of the bearing modes and the first three bending modes. As expected, the natural frequency of the bearing modes gradually increased as the rotor mass was reduced.

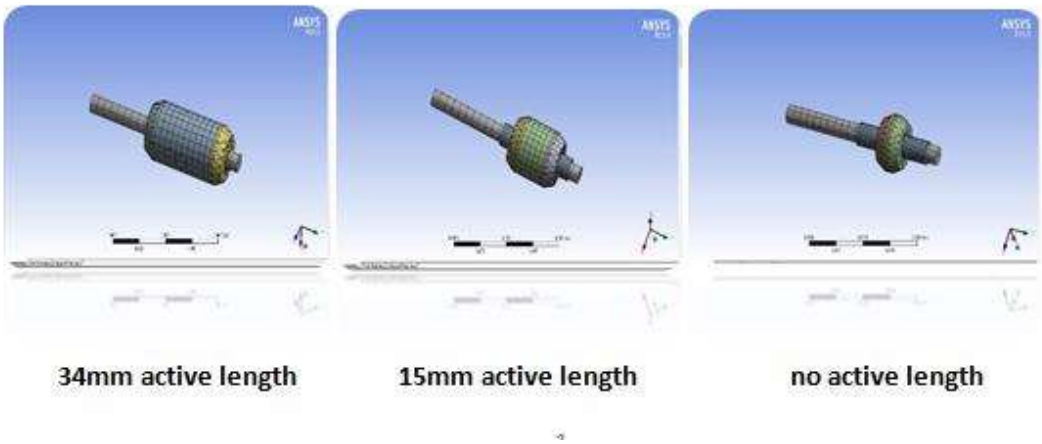

Figure (9): The Axial Length of the Active Section of the Rotor.

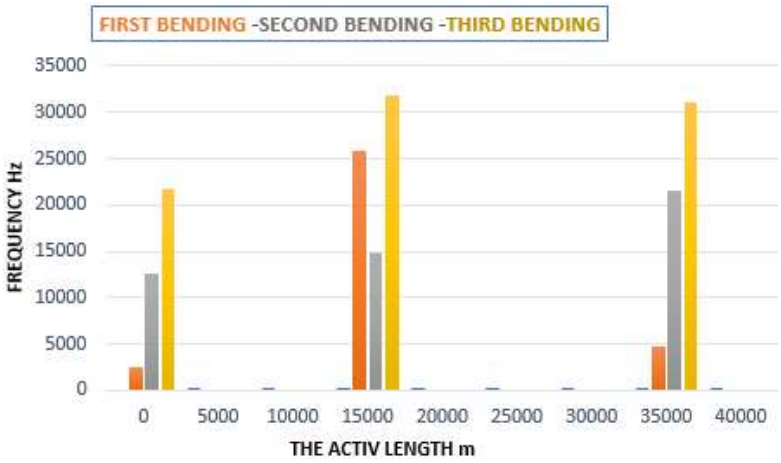

Figure (10): Different Bending Moment Mode with Different Active Length for a Shaft Length of 69mm.

The frequency of the first bending mode reduces slightly as the active length of the rotor is reduced and the rotor becomes more flexible. Regarding to the second bending mode related to the active length, as the rotor mass decreases the natural frequency initially increases. However, when the active length is reduced below 15 mm, the shaft starts to flex and the natural frequency of this mode decreases. A larger shaft diameter provides greater axial strength and, hence, increases the natural frequencies of all bending modes. However, shaft diameter will ultimately be limited by the peripheral speed capability of the bearings.

Conclusions

This paper introduces a mechanical approach to the mechanical design and characteristic analysis of a high-speed permanent-magnet synchronous motor. The analysis delivers reasonable accuracy for calculating the 1st, 2nd, and 3th bending frequencies of the permanent-magnet rotor. In order to avoid operational failure, the high-speed permanent-magnet motor designer needs to consider the rotor natural frequencies at designing stage**.** Finite Element Analysis was used to investigate the influence of the rotor geometry on its natural frequencies. It has been shown that the shaft extension has a significant influence on the natural frequencies; this leads to performing the first bending mode. It also has been shown that the rotor shaft lamination reduces the natural frequency of the rotor as it adds to the overall shaft, and little influence in axial stiffness. The magnet and inconel sleeve that has a relatively high young modulus of elasticity increases the hardness of the central of the rotor.

References

- T. J. E. Miller, Brushless Permanent-Magnet and Reluctance Motor Drive, London, U.K., Clarendon Press, 1989.

- Boldea, L. Tutelea, and C. I. Pitic, "PM-assisted reluctance synchronous motor/generator (PM-RSM) for mild hybrid vehicles: electromagnetic design," *IEEE Transactions on Industry Applications,* vol. 40, no. 2, March-April 2004, pp. 492 _498.

- Kolondzovski, Z., et al. "Rotor dynamic analysis of different rotor structures for high-speed permanent-magnet electrical machines." IET electric power applications 4.7 (2010): 516-524.

- Gardner, Joel D., Athulan Vijayaraghavan, and David A. Dornfeld. "Comparative study of finite element simulation software." (2005).

- Jason D. Ede, Z. Q. Zhu. " Rotor Resonances of High-Speed Permanent-Magnet Brushless Machines," in Industry Applications IEEE Transactions, Vol. 38, No. 6, November/December 2002.

- D. Hartog, *Mechanical Vibrations*, 4th ed. New York: McGraw-Hill, 1956.

- Longya Xu, Hongyu Wang, Han Xiong, Ziwei Ke, Julius Woo, Julia Zhang and Sheng Dong "Design and Experimental Evaluation of a High Specific Power Permanent Magnet Synchronous Machine", IEEE International Electric Machines & Drives Conference (IEMDC), 2019.

- Ayman El-Refaie and Mohamed Osama "High specific power electrical machines: A system perspective" CES Transactions on Electrical Machines and Systems, 2019 Volume: 3, Issue: 1.

- R. M. Ram Kumar;Tianjie Zou;Antonino La Rocca;Gaurang Vakil;David Gerada;Adam Walker;Chris Gerada;Krzysztof Paciura;Alastair McQueen;B. G. Fernandes "High Power High Speed PM-Assisted SynRel Machines with Ferrite and Rare Earth Magnets for Future Electric Commercial Vehicles", IECON 2019 - 45th Annual Conference of the IEEE Industrial Electronics Society, 2019.